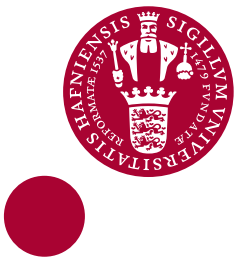

# Effects of maturation and advanced glycation on tensile mechanics of collagen fibrils from rat tail and Achilles tendons

Svensson, Rene B; Smith, Stuart T; Moyer, Patrick J; Magnusson, S Peter

*Published in:*
Acta Biomaterialia

*DOI:*
10.1016/j.actbio.2018.02.005

*Publication date:*
2018

*Document version*
Publisher's PDF, also known as Version of record

Acta Biomaterialia 70 (2018) 270–280

Contents lists available at ScienceDirect

Acta Biomaterialia

journal homepage: www.elsevier.com/locate/actabiomat

Full length article

# Effects of maturation and advanced glycation on tensile mechanics of collagen fibrils from rat tail and Achilles tendons

Rene B. Svensson [a,*], Stuart T. Smith [b], Patrick J. Moyer [c], S. Peter Magnusson [a,d]

[a] Institute of Sports Medicine Copenhagen, Department of Orthopedic Surgery M, Bispebjerg Hospital and Center for Healthy Aging, Faculty of Health and Medical Sciences, University of Copenhagen, Copenhagen, Denmark
[b] Department of Mechanical Engineering and Engineering Science, University of North Carolina at Charlotte, Charlotte, NC, USA
[c] Department of Physics and Optical Science, University of North Carolina at Charlotte, Charlotte, NC, USA
[d] Musculoskeletal Rehabilitation Research Unit, Bispebjerg Hospital, University Hospital of Copenhagen, Copenhagen, Denmark

ARTICLE INFO

*Article history:*
Received 28 September 2017
Received in revised form 24 January 2018
Accepted 6 February 2018
Available online 13 February 2018

*Keywords:*
AGE
Cross-link
Methylglyoxal
Optical marker
Pyridinoline

ABSTRACT

Connective tissues are ubiquitous throughout the body and consequently affect the function of many organs. In load bearing connective tissues like tendon, the mechanical functionality is provided almost exclusively by collagen fibrils that in turn are stabilized by covalent cross-links. Functionally distinct tendons display different cross-link patterns, which also change with maturation, but these differences have not been studied in detail at the fibril level. In the present study, a custom built nanomechanical test platform was designed and fabricated to measure tensile mechanics of individual fibrils from rat tendons. The influence of animal maturity (4 vs. 16 week old rats) and functionally different tendons (tail vs. Achilles tendons) were examined. Additionally the effect of methylglyoxal (MG) treatment in vitro to form advanced glycation end products (AGEs) was investigated. Age and tissue type had no significant effect on fibril mechanics, but MG treatment increased strength and stiffness without inducing brittleness and gave rise to a distinct three-phase mechanical response corroborating that previously reported in human patellar tendon fibrils. That age and tissue had little mechanical effect, tentatively suggest that variations in enzymatic cross-links may play a minor role after initial tissue formation.

**Statement of significance**

Tendons are connective tissues that connect muscle to bone and carry some of the greatest mechanical loads in the body, which makes them common sites of injury. A tendon is essentially a biological rope formed by thin strands called fibrils made of the protein collagen. Tendon function relies on the strength of these fibrils, which in turn depends on naturally occurring cross-links between collagen molecules, but the mechanical influence of these cross-links have not been measured before. It is believed that beneficial cross-linking occurs with maturation while additional cross-linking with aging may lead to brittleness, but this study provides evidence that maturation has little effect on mechanical function and that age-related cross-linking does not result in brittle collagen fibrils.


## 1. Introduction

In most connective tissues the primary load bearing function is provided by fibrillar collagens [1]. Collagen fibrils can form spontaneously through non-covalent interactions by an organized staggered aggregation of collagen molecules [2,3]. The mechanical function of the fibrils and the tissues they form is believed to depend on stabilization by covalent bonds called cross-links that result from the activity of lysyl oxidase enzymes (LOX) [4–6]. The cross-links are formed in several steps; initially so-called immature divalent bonds are formed, which can subsequently react further to form different mature, trivalent bonds [7,8]. The mature forms are stable to acids, while the immature cross-links

*Abbreviations:* AFM, atomic force microcopy; AGE, advanced glycation end product; HYP, hydroxyproline; HP, hydroxylysyl pyridinoline; LP, lysyl pyridinoline; MG, methylglyoxal; PBS, phosphate buffered saline.

* Corresponding author at: Institute of Sports Medicine Copenhagen, Bispebjerg Hospital 8.1, Bispebjerg Bakke 23, 2400 Copenhagen NV, Denmark.
*E-mail addresses:* rbs@nano.ku.dk, svensson.nano@gmail.com (R.B. Svensson).

https://doi.org/10.1016/j.actbio.2018.02.005
1742-7061/

come in a stable ketoamine form and an acid labile aldimine form [9].

In addition to the enzymatic cross-links, reducing sugars (e.g. glucose) and certain metabolic products (e.g. methylglyoxal) can react with proteins to produce various adducts, some of which form cross-links [10,11]. The final products of such reactions are called advanced glycation end products (AGEs), which accumulate over time on long-lived proteins like collagens. A glucose derived cross-linking AGE called glucosepane is currently believed to be the major species accumulating on matrix proteins in vivo [12–14]. Two methylglyoxal derived cross-links called MODIC and MOLD have also been reported in vivo but at lower concentrations [12–14]. Glucosepane and MODIC are both lysine-arginine cross-links while MOLD links two lysines. The three cross-links are of similar length but glucosepane is more bulky [13]. Unlike enzymatic cross-links, AGE formation can take place at multiple different sites along the helical region of collagen molecules [15,16]. Glucosepane and MODIC are likely to form at the same sites, with 8 potential intermolecular lysine-arginine pairs having been reported, in contrast MOLD may be more likely to form intramolecular bonds due to the proximity of lysine residues on the two identical alpha chains within the type I collagen molecule [16].

Enzymatic and AGE cross-links both contribute to the chemical stability of collagen [17,18], and tissues tend to get mechanically stronger with maturation, and weaker with inhibition of enzymatic cross-links [19,20]. Induction of AGEs in vitro has also been associated with increased stiffness and strength [21,22], although in vivo findings are inconsistent [23–26]. Glycation is thought to be detrimental to tissue function with brittleness and reduced strain capacity [27], but there is little such evidence at the tissue level [22]. However, brittleness may still be present at the fibril level, which could result in fragmentation of the fibrils and thereby help explain the reduced stiffness with aging.

Macroscopic mechanical properties can be affected by mechanisms operating at different levels of the structural hierarchy, but the influence of cross-links is expected to occur at the scale of individual collagen fibrils, although this has never been conclusively demonstrated. Mechanically testing individual fibrils is possible, albeit technically challenging [28–32]. Absolute mechanical properties vary significantly between previous studies, but there is general agreement that type I collagen fibrils display intrinsic viscoelasticity [33–35]. Increased stiffness and strength have been reported from different synthetic cross-links [35], but the influence of naturally occurring enzymatic and AGE cross-links has not been studied directly. Indirect measurements using x-ray diffraction have shown that deficiency in enzymatic cross-links resulted in reduced strength and stiffness [36], and that induction of AGEs in vitro led to an increase in strength and strain without a change in stiffness [37]. The x-ray diffraction technique is limited by failure of the macroscopic specimen, which may occur by mechanism unrelated to fibril ultimate properties, and because details in the fibril mechanical response may be blurred by averaging across a large number of fibrils.

The present study aimed to investigate how enzymatic and AGE cross-links affect fibril mechanics by studying the influence of animal maturation using immature (4 week old) and mature (16 week old) rats, and functionally different tendons using tail and Achilles. These factors relate indirectly to enzymatic cross-linking since animal maturation is associated with cross-link maturation [27], and tail tendons are more acid labile than Achilles indicating lower levels of stable immature and mature cross-links [38]. Samples were treated with methylglyoxal (MG) in vitro to mimic AGE formation at a supraphysiological level. A new mechanical device was designed to investigate strain distribution along the fibril during mechanical testing since fibril deformation may not be uniform [39]. We hypothesized the following: *a*) mature enzymatic cross-linking would be greater in old compared to young rats, and greater in Achilles compared to tail tendons, *b*) the stiffness and strength of collagen fibrils would increase with increasing mature enzymatic cross-linking, *c*) AGE induction by methylglyoxal would increase stiffness and strength but decrease ultimate strain, resulting in more brittle collagen fibrils, and *d*) strain within fibrils would be localized in distinct regions but become more uniform with increased cross-linking.

## 2. Materials and methods

### 2.1. Materials

Hind limbs and tails from 4 and 16 week old male Wistar rats were obtained from Charles River (6 at each age). Individual fascicles (macroscopic tendon subunits) were extracted from the tails by cutting the distal end and pulling fascicles with tweezers (Fig. 1). Only the two larger ventral bundles were used. In addition, the free length of Achilles tendon was dissected from the hind limbs. A single tail fascicle was obtained for fibril mechanics, and divided transversely with one half treated with MG (Section 2.2). Two fascicles were taken for macroscopic mechanical testing and they were divided transversely with one distal and one proximal part treated with MG. Several additional fascicles were extracted and separated into small bundles (~5 mg) for acid solubility, fluorescence and cross-link measurements. Each bundle was divided transversely and one half randomly assigned to MG treatment. Each Achilles tendon was cut into three longitudinal strips and divided transversely to get 6 pieces. The pieces were randomly assigned with two for fibril mechanics and cross-links, two for acid solubility and two for fluorescence, half of which were treated with MG.

### 2.2. Methylglyoxal treatment

Half of the samples were treated with MG to induce AGEs in a similar way as previously published by Li et al [40]. Treatment was performed in a buffer of 100 mM EPPS (4-(2-hydroxyethyl)-1-piperazinepropanesulfonic acid, E1894, Sigma-Aldrich), 150 mM phosphate buffered saline (PBS) and 5 mM EDTA adjusted to pH 8.5. Control samples were treated with just the buffer and glycated samples with the buffer including 20 mM MG (W296902, Sigma-Aldrich). Each sample was treated in 1 mL solution at 36 °C for 4.5 h. Following treatment, tissue was washed and stored frozen (−20 °C) in PBS. Fascicle mechanics and fluorescence were measured within 3 months but due to time consuming method development, fibril measurements were conducted after 2–3 years and, for the sake of comparability, acid solubility and cross-links were measured in this period as well.

### 2.3. Acid solubility

Chemical stability of collagen was assessed by acid solubility [41]. Tissue pieces (~1 mg wet weight) were lightly blotted to remove excess liquid, finely minced with a scalpel and dissolved in 1 mL of 50 mM acetic acid for 20 h (4 °C) with light agitation. Samples were centrifuged at 24000*g* for 1 h (4 °C) and separated by taking 0.5 mL of the supernatant and leaving the remaining 0.5 mL of supernatant with the pellet to minimize disruption. Supernatant and pellet samples were hydrolyzed by adding 0.5 mL of 12 M HCl to each (6 M final concentration) and boiling at 110 °C over night in a tightly sealed polypropylene tube (Safe-T-Seal, 1420–9701, USA Scientific Inc.). Hydrolyzed samples were dried on a heat block at 95 °C, washed with 1 mL of distilled water and dried again. As a measure of collagen content, the collagen "specific" amino acid

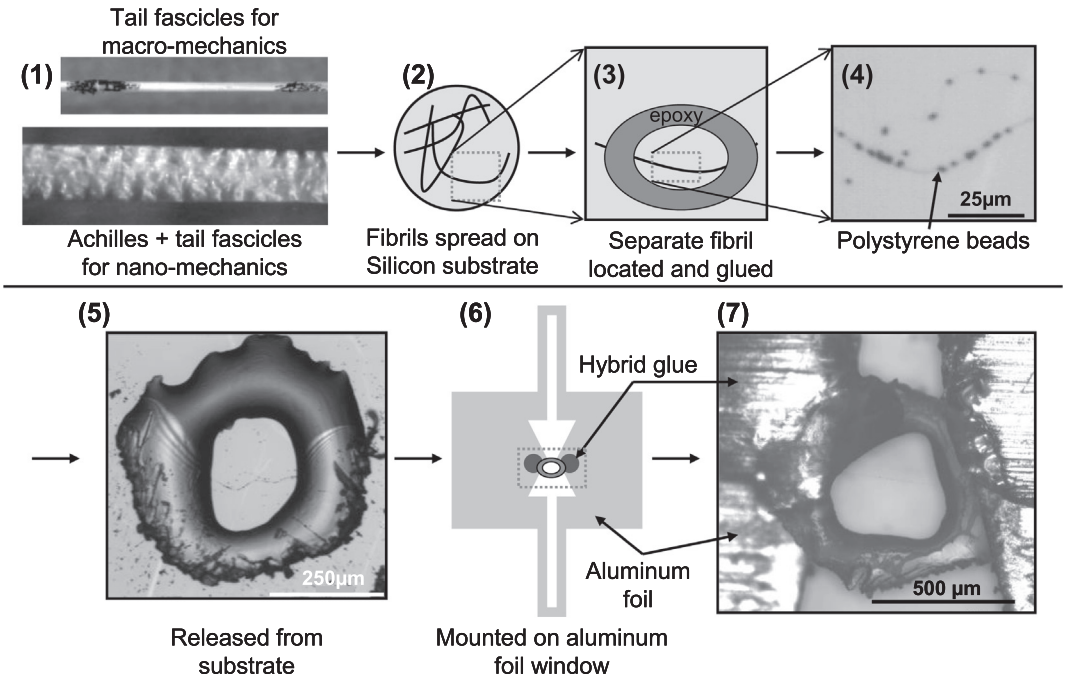


**Fig. 1.** Schematic of fibril sample preparation (Section 2.7 for details). 1) Achilles and tail tendon fascicles taken for fibril testing. Tail fascicles were also prepared for macroscopic mechanical testing with ink marks. 2) Fibrils spread onto a silicon substrate. 3) A separate fibril is enclosed by a ring of epoxy glue. 4) Polystyrene spheres adsorbed to fibril for optical tracking. 5) Epoxy ring is partly released from substrate. The detached (bottom) part of the ring appears brighter with scratches from the scraping, while the top part is still attached and appears darker. 6) Epoxy ring with fibril is mounted in the opening of an aluminum foil window. Just before mechanical testing the two wings (pointing up and down) are cut. 7) Microscopy image of the sample on the window.

hydroxyproline (HYP) was determined according to a colorimetric assay based on 4-dimethylaminobenzaldehyde (method details in Supplement S1.1) [42]. Solubility was determined as the HYP content in the supernatant divided by the total HYP content in the pellet and supernatant.

### 2.4. Fluorescence

Several of the products formed by glycation are fluorescent [43], and total fluorescence can be used as an indirect measure of AGE modification [44,45]. Tissue was hydrolyzed and as a measure of collagen content, HYP was determined in an aliquot by the assay mentioned above (Supplement S1.1). Aliquots of the remaining hydrolysate were diluted 1, 5, 25 and 125 fold in an acetate-citrate buffer used for the HYP assay (0.55 M acetate, 0.13 M citrate, pH 6.0). Samples (200 µL) were added to the wells of a 96-well plate and fluorescence measured (CytoFluor4000, Applied Biosystems) at wavelengths 360/40 nm (excitation) and 460/40 nm (emission). A plateau effect could be seen for some of the high concentration samples and only values with a linear relation to concentration were used. Fluorescence values were normalized to HYP content.

### 2.5. Enzymatic cross-links

Mature enzymatic pyridinoline cross-links, hydroxylysyl pyridinoline (HP) and lysyl pyridinoline (LP), were evaluated by HPLC. Samples (~2 mg) underwent gas-phase hydrolysis for 24 h at 110 °C using 37% HCl containing 0.3% phenol. Air was removed from the hydrolysis vessel by three consecutive applications of vacuum and nitrogen, ending with vacuum. Resulting hydrolysates were vacuum dried at room temperature over night, re-dissolved in 2 M HCl and aliquots containing approximately 0.3 mg sample were taken for analysis. Aliquots were vacuum dried and re-dissolved in 75 µL of 1% heptafluorobutyric acid (HFBA) containing an internal standard of 2 µM pyridoxamine dihydrochloride. Separation was on a reversed phase column (Kinetex 2.6 µm C18 100 Å, Phenomenex) using a non-linear decreasing gradient (91%–77.6%) of eluent A (25 mM $NH_4OH$, 10 mM HFBA (pH 2.4)) against eluent B (25% eluent A, 75% acetonitrile with 10 mM HFBA). Quantification was based on standards of HP and LP (PYD/DPD HPLC Calibrator, 8004, Quidel Corp.).

### 2.6. Fascicle mechanics

Fascicles were marked with a black pen at two locations (~2 mm apart) for optical strain tracking. Ink did not enter the fascicle but formed a dry "crust" on the surface. Fascicles were glued with cyanoacrylate at a nominal gauge length of 20 mm onto the clamps of a microtensile tester (200-N tensile stage, petri dish version, Deben) equipped with a 20 N load cell. The glue cured for 30 min while the free part of the fascicle was hydrated by a strip of PBS soaked tissue paper. Samples were loaded to an onset force of 0.01 N for 4-week old tails and 0.05 N for 16-week old tails (due to their larger diameter) followed by 10 cycles of preconditioning to 1.5% strain. The fascicle was loaded to the onset point and the width and thickness (using a 45° mirror) measured on microscope images at three locations. Finally the sample was loaded to failure with simultaneous video recording (18 Hz) for use in optical strain tracking. All tests were conducted at a speed of 4 mm/min. Tracking of optical strain markers was performed using the "Tracker" open-source software [46]. Optical and mechanical data were manually synchronized to the start of motor movement and the failure point. Modulus was determined as the peak value of a moving linear fit over a 1% strain window.

### 2.7. Fibril mechanics

See Fig. 1 for a schematic overview of the sample preparation. A 1 mm long piece of a single fascicle was divided longitudinally and the exposed surface sheared across a silicon substrate under a droplet of PBS. The sample was rinsed in distilled water and blown

dry with nitrogen. Suitable fibrils (separate from other fibrils and >100 μm long) were located in an optical microscope with dark-field illumination. Using a thin hair, a ring of two-component epoxy glue (Epoxy Extra Strong, Bostik) was placed around the fibrils to just cover the ends. The epoxy cured at ambient conditions for at least 24 h, and then a 20 μL droplet of 1 μm polystyrene beads (Polybead Microspheres, Polysciences Inc) diluted to 0.625 mg/mL in PBS was placed on the sample for 15 min to adsorb optical markers onto fibrils for strain analysis (Fig. 2A). The sample was rinsed with distilled water and blown dry with nitrogen. A central part of each fibril was imaged with atomic force microscopy (AFM) to determine the dry cross-sectional area as previously described [47]. Finally the epoxy ring holding the fibril was released from the surface by scraping with the tip of a 27 gauge syringe needle. The ring was picked up with negative action tweezers and attached to an aluminum foil "window" (Fig. 1) (50 μm thick) using hybrid glue (Universal Hybrid Glue, Loctite) applied with a thin hair. Using a laser microdissection microscope (Axio Observer Z1, Zeiss) the epoxy ring was cut open, and then the aluminum foil window was mounted on the custom built nanomechanical test device. A detailed description of the device can be found in the Supplementary material (S1.2). In brief, the device uses a piezoelectric actuator to apply deformation and a macroscopic cantilever together with a capacitance sensor to measure force. The device can be mounted on an inverted microscope to observe the fibril and measure strain optically. Using a chamber slide, the sample can be immersed in liquid. The sample was attached to the device using cyanoacrylate glue (Super Glue Precision, Loctite), which cured for 30 min. The "wings" of the aluminum window were cut with a micro-scissor and the device was placed on the microscope with the sample immersed in PBS. After hydrating for ~30 min the fibril was gently stretched until a minimal force was detected, and then a single linear ramp to failure was performed. The average strain rate was 3.6%/s and varied (SD 1.2%/s) due to differences in fibril length. Because the fibril was slack when immersed in PBS, it would move around and often adsorb to the edges of the clamp. During the ramp to failure it would then detach at low force and once again get slack. In these cases the test was stopped, the fibril was again stretched until almost taut and another ramp to failure was performed.

### 2.8. Fibril data analysis

Optical markers on the fibrils were tracked using a custom Matlab routine (MATLAB R2015b, MathWorks Inc.) based on cross-correlation (Fig. 2A). To the extent possible a minimum spacing between tracking points of 50 pixels (~18 μm) was maintained to reduce the strain measurement error, and consequently not all optical markers were tracked on each fibril. To assess tracking quality, pixel positions were high-pass filtered by subtracting a moving average over 10 points (~1 s) and determining the standard deviation of the remaining noise. Typical noise values were between 0.2 and 1 pixel for stationary and fast moving points respectively (points closer to the actuator move faster than points near the stationary cantilever). The frame rate was not constant during the microscope video recordings and as a result they could not be directly synchronized to the mechanical data. To overcome this issue, a point solidly connected to the piezo actuator was tracked in the video and the movement of this point expressed relative to its total movement during the ramp. The same relative motion from the piezo position sensor was also determined for the ramp and the two data sets were synchronized (i.e. the frame in which the video showed a relative piezo movement of X%, was synchronized to the mechanical data where the position sensor also reached X% of the total range).

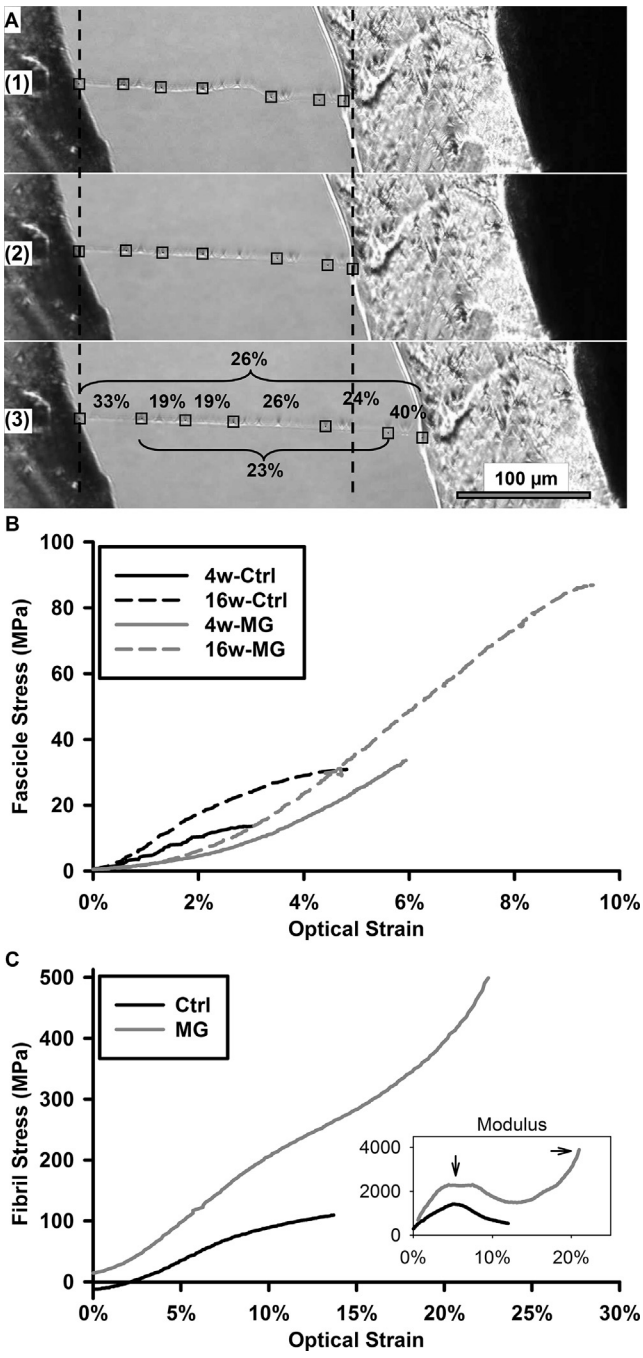


**Fig. 2.** A) Example optical strain tracking on a collagen fibril. Left and right sides are the cantilever and piezo actuator respectively. Square boxes show the tracked regions. (1) Slack fibril. (2) Taut fibril at the onset of force. (3) Last frame before failure, showing the total strain, regional strains and strain excluding the ends. B) Example stress-strain curves from fascicles with different age and treatment. C) Example stress-strain curves from collagen fibrils with and without methylglyoxal treatment. The onset deviates from zero stress because of baseline drift (details in Supplement S1.2). Inset shows the modulus along the curves with arrows at the first and second peak in the MG sample. Ctrl = untreated, MG = methylglyoxal treated.

Optical deformation data (~10 Hz) was upsampled and synchronized to the mechanical data (400 Hz), and all the data was filtered with a 40 point (0.1 s) wide moving average and finally downsampled to 40 Hz before further analysis. Peak elastic modulus was determined as the first peak value of a moving linear fit over a 3% strain window (Fig. 2C inset). As described later, some

fibrils displayed a secondary peak in modulus, but the value denoted as "peak modulus" throughout refers only to the first peak which is present in all samples. Note that all stress-related measurements (stress and modulus) are based on dry fibril cross-sectional areas.

### 2.9. Statistics

Fascicle mechanical parameters were averaged across duplicate samples from each animal before statistical analysis. In contrast, fibril mechanical data was not averaged across animals because it is the individual fibril responses that are of interest in this study. Since the study had a full factorial design (2x2x2), a three-way ANOVA (generalized linear model) was used with Tukey-Kramer adjusted post tests. Initially, all interactions were included in the analysis, if the third-order interaction was not significant it was removed and the analysis repeated. Any of the three second-order interactions that were not significant were removed and the analysis repeated with the final model containing all the main effects and any remaining significant interactions. Several of the mechanical parameters showed a log-normal residual distribution and since the remaining parameters were also well represented by a log-normal distribution, all the mechanical data was log transformed. Results are shown as back-transformed geometric means and geometric standard errors. All parametric analyses were performed in SAS (v.9.2, SAS Institute Inc.).

For the enzymatic cross-link measurement, one group had zero HP content in all measurements, making parametric statistics unsuitable. Instead separate rank-based Mann-Whitney U tests were performed on the effect of age within each tissue and the tissue difference at each age with Bonferroni correction for the four comparisons (Prism 7, GraphPad software Inc.). For the sake of comparability, the same analysis was made for the LP cross-links.

## 3. Results

Group comparisons are presented as mean values (geometric means for mechanical data) within the compared groups across any uninvolved factors (i.e. for a main effect of treatment the mean value of each treatment group is taken across all ages and tissue types). Individual group values and standard errors are reported in tables and figures. Tables displaying confidence intervals and main effects of age, treatment and tissue type on fascicle and fibril mechanics can be found in the Supplement (Tables S1–S3).

### 3.1. Acid solubility

MG treatment resulted in completely insoluble samples (the values shown represent the detection limit of the measurement) (Fig. 3A). Since the Achilles tendons had lower solubility than the tails, there was a two-way interaction between tissue type and treatment ($p < 0.0001$), showing that the reduction with treatment was smaller in the Achilles (9.1% vs. 0.3%, $p < 0.05$) (control vs. treated) than in the tail (91.7% vs. 0.5%, $p < 0.0001$). Because acid solubility of treated samples was at the detection limit in all groups, the effects of age and tissue type were only assessed in untreated samples. There were no interactions between age and tissue type, but there was an effect of tissue type with Achilles tendons having significantly lower acid solubility than tails (9.1% vs. 91.7%, $p < 0.0001$). Acid solubility was not significantly affected by age, but tended to be lower in the older animals (46.9% vs. 54.0%, $p = 0.07$).

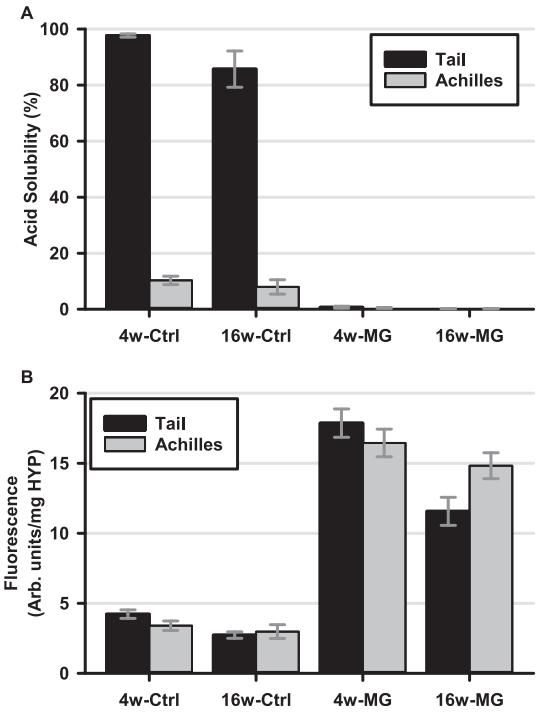


**Fig. 3.** A) Solubility of tendon collagen samples in 50 mM acetic acid. B) Fluorescence of tendon hydrolysates as indicator of AGE formation. Ctrl = untreated, MG = methylglyoxal treated, HYP = hydroxyproline. Mean and SE.

### 3.2. Fluorescence

Fluorescence values are shown in Fig. 3B. There were two-way interactions between age and tissue type ($p < 0.01$) as well as age and treatment ($p < 0.005$). Analyzing these interactions showed that fluorescence was not affected by age in the Achilles tendon (9.9 vs. 8.9, $p = 0.47$) (4 week vs. 16 week) but reduced with age in the tail tendons (11.1 vs. 7.2, $p < 0.0001$), and also that there was no effect of age in controls (3.8 vs. 2.9, $p = 0.52$) but a reduction with age in MG treated samples (17.2 vs. 13.2, $p < 0.0001$) (see discussion in Supplement S2.1). There was a significant increase with MG treatment across tissues at both 4 weeks (3.8 vs. 17.2, $p < 0.0001$) and 16 weeks (2.9 vs. 13.2, $p < 0.0001$).

### 3.3. Enzymatic cross-links

Cross-link values for the untreated samples are shown in Table 1. The concentration of HP was significantly higher in the Achilles compared to the tail at both 4 weeks (90 vs. 0 mmol/mol, $p < 0.01$) and 16 weeks (278 vs. 2 mmol/mol, $p < 0.01$). HP also increased with age in both tails (0 vs. 2 mmol/mol, $p < 0.01$) and Achilles (90 vs. 278 mmol/mol, $p < 0.05$). For LP there was a significant increase with age in the tail (8 vs. 21 mmol/mol, $p < 0.01$) but no significant differences between any of the other groups.

### 3.4. Fascicle mechanics

Mechanical properties of tail fascicles using optical strain are shown in Fig. 2B, Fig. 4A-C and Table 2. All mechanical parameters increased with both age and MG treatment. Failure stress increased with age (20 vs. 51 MPa, $p < 0.0001$) and MG treatment (20 vs. 50 MPa, $p < 0.0001$). Failure strain increased with age (3.8% vs. 6.7%, $p < 0.001$) and MG treatment (3.5% vs. 7.3%, $p < 0.0001$). Failure energy increased with age (0.3 vs. 1.3 MJ/m$^3$, $p < 0.0001$) and MG treatment (0.3 vs. 1.4 MJ/m$^3$, $p < 0.0001$). Peak modulus increased

**Table 1**
Enzymatic cross-links normalized to molar collagen content. Median [1st-3rd quartile] (N).

| | | Tail 4 week | Tail 16 week | Achilles 4 week | Achilles 16 week |
|---|---|---|---|---|---|
| HP (mmol/mol) | Ctrl | 0 [0–0] (6) | 2 [1–4] (6) | 90 [70–106] (5) | 278 [153–326] (6) |
| LP (mmol/mol) | Ctrl | 8 [7–8] (6) | 21 [13–27] (6) | 12 [1–13] (5) | 13 [10–19] (6) |

Ctrl = untreated.

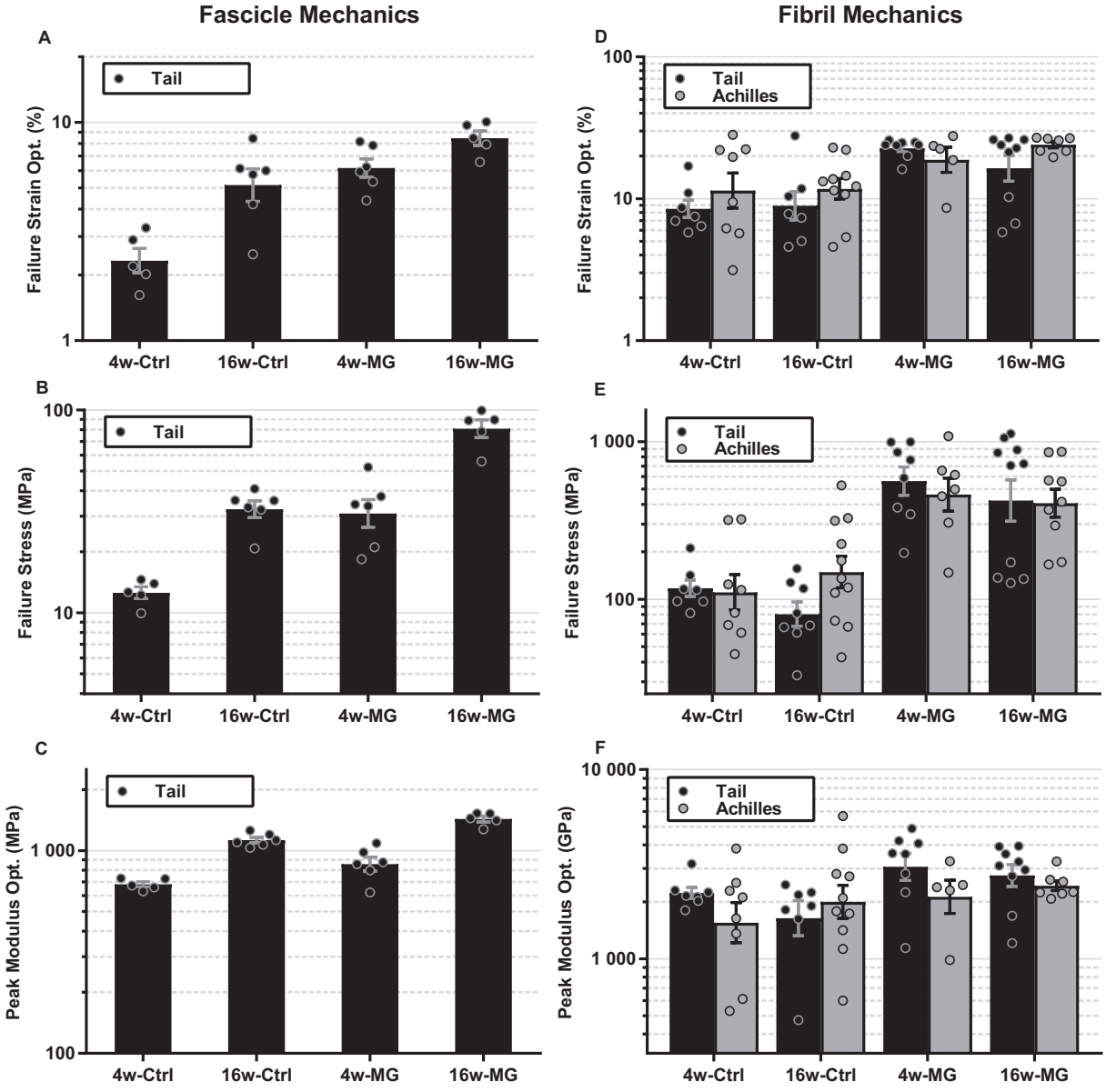


**Fig. 4.** Mechanical data. A, B, C) Failure strain, stress and peak modulus for fascicles. Based on optical strain measurement. D, E, F) Failure strain, stress and peak modulus for fibrils. Based on optical strain measurement. Ctrl = untreated, MG = methylglyoxal treated. Geometric mean and geometric SE.

with age (0.77 vs. 1.27 GPa, $p < 0.0001$) and MG treatment (0.88 vs. 1.11 GPa, $p < 0.0005$). There were no interactions, indicating that the age difference remained the same after MG treatment. Nominal failure strain was significantly greater than optical failure strain (6.7% vs. 5.1%, $p < 0.0001$), but the mechanical properties behaved similarly regardless of using optical or nominal strain, except that the increase in modulus with MG treatment was not significant using nominal strains.

Fascicle diameter increased significantly with age (0.13 vs. 0.22 mm, $p < 0.0001$) but not with MG treatment. The tested segment length was significantly greater in the 4-week old MG treated group than any of the other groups ($p < 0.005$). This was due to contraction after MG treatment resulting in a bit of curling (the thicker 16-week old fascicles were less prone to curl). To investigate if differences in diameter and length could underlie some of the mechanical group differences the linear model was extended

**Table 2**
Fascicle mechanics from optical strains in the central region. Geometric mean [geometric SE] (N).

| | | Tail 4 week | Tail 16 week |
|---|---|---|---|
| Length (mm) | Ctrl | 22.2 [22.0–22.4] (5) | 21.9 [21.6–22.3] (6) |
| | MG | 24.4 [24.0–24.8] (6) | 21.8 [21.6–22.0] (5) |
| Diameter (mm) | Ctrl | 0.13 [0.11–0.15] (5) | 0.21 [0.17–0.25] (6) |
| | MG | 0.14 [0.12–0.17] (6) | 0.23 [0.19–0.29] (5) |
| Failure Stress (MPa) | Ctrl | 13 [12–13] (5) | 32 [29–36] (6) |
| | MG | 31 [26–36] (6) | 81 [73–89] (5) |
| Failure Strain (%) | Ctrl | 2.3 [2.0–2.6] (5) | 5.2 [4.3–6.1] (6) |
| | MG | 6.2 [5.6–6.8] (6) | 8.5 [7.8–9.1] (5) |
| Failure Energy (MJ/m$^3$) | Ctrl | 0.2 [0.1–0.2] (5) | 1.0 [0.7–1.3] (6) |
| | MG | 0.7 [0.5–0.9] (6) | 2.9 [2.4–3.5] (5) |
| Peak Modulus (GPa) | Ctrl | 0.68 [0.66–0.70] (5) | 1.13 [1.10–1.16] (6) |
| | MG | 0.86 [0.79–0.93] (6) | 1.43 [1.39–1.48] (5) |

Ctrl = untreated. MG = methylglyoxal treated.

by including diameter and length. Doing so did not change the results, except the effect of age on failure strain did not achieve statistical significance, but the magnitude of the effect remained the same.

### 3.5. Local fibril strains

Of the 68 fibrils tested in this study 61 were successfully marked with polystyrene beads for optical strain analysis (Table 3). The ends were observed to strain substantially more than the central region (20.6% vs. 14.1%, $p < 0.0001$) (Fig. 2A), which was likely due to end-effects resulting from an imperfect interface to the sample [48]. Therefore, the remaining analyses were performed only on optical markers in the central region. Since the strain at the ends was increased, the failure strain in the central region was necessarily reduced from the nominal value (14.1% vs. 16.2%, $p < 0.0001$) and modulus calculated from optical strain was consequently increased (2.2 vs. 1.9 GPa, $p < 0.0001$). Uniformity of the strain distribution was assessed by the standard deviation of strains within the central region of each fibril. This standard deviation was not dependent on the age, tissue or treatment group. At the failure point the standard deviation was 2.1%, which is 15% of the total strain (14%) at that point. The average segment length between two tracking points was 105 pixels, which means that the ~1 pixel tracking noise could account for about 1% variation in strain.

Failure strain at the local site where rupture occurred was significantly increased compared to the mean optical failure strain in the central region (16.8% vs. 15.1%, $p < 0.05$) (discarding 25 (41%) tests where failure occurred in the end regions and an additional 2 (3%) tests where the number of strain markers was too low (<5) to differentiate local strains within the central region).

### 3.6. Fibril mechanics

Mechanical properties are reported using optical strain in the central region (Fig. 2C, Fig. 4D–F, Table 3). None of the fibril mechanical parameters were affected by age or tissue type, and there were no significant three- or two-way interactions. However, all of the mechanical parameters increased significantly with MG treatment. Failure stress increased with MG treatment (110 vs. 460 MPa, $p < 0.0001$). Failure strain increased with MG treatment (10.1% vs. 20.5%, $p < 0.0001$). Failure energy increased with MG treatment (7 vs. 40 MJ/m$^3$, $p < 0.0001$). Peak modulus increased with MG treatment (1.9 vs. 2.6 GPa, $p < 0.05$). Using nominal strain, group differences in mechanical parameters were equivalent to those using the optical strain (i.e. no effect of age or tissue, but a significant effect of MG treatment) (Table S4 in Supplement).

Fibril diameter varied across the groups, which resulted in a statistically significant three-way interaction ($p < 0.005$) (Fig. 5A). There was no direct correlation between diameter and any mechanical properties, but adding diameter to the linear model showed a significant reduction of failure stress ($r^2$ (semi-partial) = 0.05, $p < 0.01$) and peak modulus ($r^2$ (semi-partial) = 0.09, $p < 0.01$) with increasing diameter (Fig. 5B). Inclusion of diameter in the ANOVA model did not change the effects of age, tissue type and MG treatment.

A three-phase mechanical response that consisted of an initial region of high modulus, followed by a plateau region of low modulus leading to a second region of high modulus (Fig. 2C), was present in 26 of the 34 MG treated fibrils (76%) and 2 of the 34 untreated fibrils (6%). Since few control fibrils displayed this behavior, the effects of age and tissue type were only assessed in

**Table 3**
Fibril mechanics based on optical strains in the central region. Geometric mean [geometric SE] (N).

| | | Tail 4 week | Tail 16 week | Achilles 4 week | Achilles 16 week |
|---|---|---|---|---|---|
| Length (μm) | Ctrl | 144 [127–163] (7) | 267 [240–298] (8) | 231 [217–245] (8) | 223 [200–248] (11) |
| | MG | 202 [183–224] (8) | 270 [243–299] (10) | 202 [176–232] (7) | 187 [168–209] (9) |
| Dry Diameter (nm) | Ctrl | 143 [137–150] (7) | 231 [209–255] (8) | 110 [104–116] (8) | 153 [146–161] (11) |
| | MG | 162 [151–174] (8) | 180 [168–193] (10) | 130 [121–141] (7) | 201 [190–212] (9) |
| Failure Stress (MPa) | Ctrl | 120 [100–130] (7) | 80 [70–100] (8) | 110 [90–140] (8) | 150 [120–190] (11) |
| | MG | 560 [460–690] (8) | 420 [310–570] (10) | 460 [360–590] (7) | 410 [330–500] (9) |
| Failure Strain, Ends (%) | Ctrl | 18 [15–21] (7) | 20 [16–25] (7) | 13 [10–16] (8) | 14 [11–18] (10) |
| | MG | 31 [28–34] (8) | 23 [19–28] (9) | 23 [20–26] (5) | 37 [31–45] (7) |
| Failure Strain, Central (%) | Ctrl | 8.5 [7.4–9.8] (7) | 8.9 [7.1–11.2] (7) | 11.5 [8.6–15.3] (8) | 11.7 [10.0–13.9] (10) |
| | MG | 22.9 [21.7–24.2] (8) | 16.2 [13.2–20.0] (9) | 19.1 [15.5–23.4] (5) | 24.0 [22.9–25.2] (7) |
| Failure Energy (MJ/m$^3$) | Ctrl | 6 [5–8] (7) | 5 [4–6] (7) | 6 [4–10] (8) | 10 [6–14] (10) |
| | MG | 56 [46–67] (8) | 29 [18–46] (9) | 29 [20–44] (5) | 46 [39–55] (7) |
| Peak Modulus (GPa) | Ctrl | 2.2 [2.1–2.4] (7) | 1.6 [1.3–2.0] (7) | 1.6 [1.2–2.0] (8) | 2.0 [1.6–2.4] (10) |
| | MG | 3.1 [2.6–3.6] (8) | 2.8 [2.4–3.1] (9) | 2.1 [1.7–2.6] (5) | 2.4 [2.3–2.6] (7) |
| 2nd Peak Modulus (GPa)[a] | Ctrl | (0) | (0) | 0.8 [–] (1) | 2.6 [-] (1) |
| | MG | 5.9 [4.1–8.4] (6) | 6.0 [3.5–10.3] (6) | 3.2 [2.7–3.9] (4) | 4.7 [3.3–6.8] (6) |
| Strain SD within Fibrils (%)[b] | Ctrl | 1.8 [1.3–2.4] (6) | 1.3 [1.0–1.9] (7) | 1.3 [0.8–2.1] (8) | 2.4 [1.8–3.1] (10) |
| | MG | 2.3 [1.8–3.0] (8) | 1.6 [1.2–2.2] (9) | 1.6 [1.0–2.4] (4) | 1.5 [1.2–2.0] (5) |

Ctrl = untreated. MG = methylglyoxal treated.
[a] Only including samples that had the three-phase behavior.
[b] Standard deviation (SD) of local strains within the central region of each fibril. Sample sizes are reduced because some samples only had enough strain markers (4) to measure one local strain in the central region and therefore no SD could be determined.

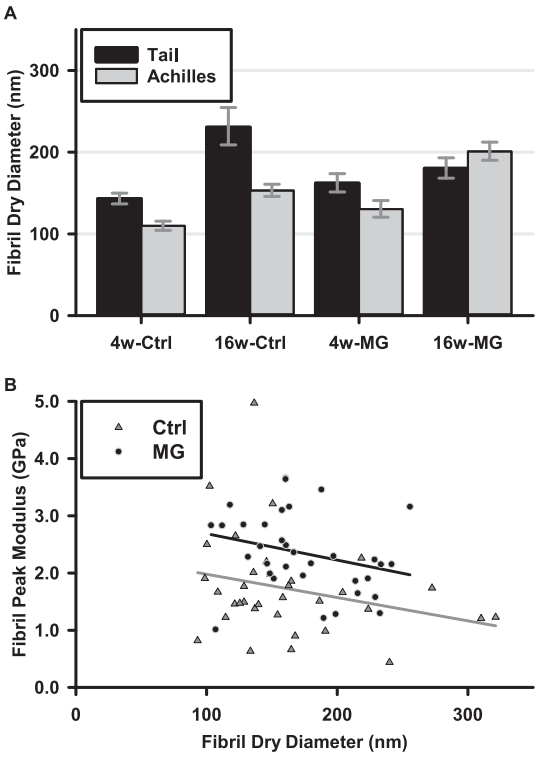


**Fig. 5.** Fibril diameter. A) Fibril diameter in each group. Mean and SE. B) Relation between fibril peak modulus and fibril diameter. These correlations were not directly significant, only after accounting for all group differences (Section 4.3 for details). Ctrl = untreated, MG = methylglyoxal treated.

the treated samples. Age and tissue type had no effect on either the second peak modulus or the ratio between the second and first peak modulus, but the second peak modulus was greater than the first (4.1 vs. 2.3 GPa, $p < 0.0001$).

## 4. Discussion

Functionally distinct tendons have different mechanical requirements, and mechanical function also develops during maturation. Differences in naturally occurring cross-links often accompany differences in tissue type and maturation and could be an important contributor to mechanical function at the fibril level. The differences in acid solubility and mature enzymatic HP cross-links in the present tissues suggest variations in cross-link profile that could affect fibril mechanics. MG treatment also successfully modified the collagen as evidenced by the loss of solubility and rise in fluorescence.

### *4.1. Animal maturity and tendon type*

Since cross-links are located between collagen molecules within a collagen fibril they are expected to exert the strongest influence on the fibril, with the effect getting attenuated at higher levels of the structural hierarchy up to the macroscopic tendon. In contrast, we have previously shown that treatment of tendon with $NaBH_4$, which chemically stabilizes immature enzymatic cross-links, had a notable mechanical effect at the fascicle level, but not at the level of individual fibrils [31]. Similarly, in the present study mechanical properties of tail fascicles greatly increased in the more mature animals, while individual fibrils were unaffected in spite of higher HP concentration. This suggests that changes at the macroscopic level did not originate in the material properties of fibrils but may instead involve mechanisms such as increased fibril length or interconnectedness. In addition, there were no significant differences in the behavior of fibrils from tail and Achilles tendons in spite of their different functional roles at the macroscopic level. The high acid solubility of tails, especially in the immature animals, indicates a low level of stable mature and immature cross-links. The lower solubility in Achilles tendons indicates a greater concentration of stable cross-links and the higher content of HP suggests that some of these are mature ketoamine cross-links. These results indicate that fibrils from functionally different tendons do not behave differently, in spite of differences in chemical stability and enzymatic cross-links. It is possible that labile immature enzymatic cross-links are sufficient to provide mechanical reinforcement, and non-labile and mature cross-links mainly contribute to increasing chemical and not mechanical stability. It should be noted that mechanical properties had a high variance, which could mask some of the difference. The 95% confidence interval would for example allow the Achilles fibrils to have between 20% lower and 54% higher stress than those from the tail (see Supplementary Tables S1–S3).

### *4.2. Methylglyoxal treatment*

MG treatment significantly increased all measured mechanical properties at both the fascicle and fibril level. The relative magnitude of the increase was similar in fibrils and fascicles, although the peak modulus, failure stress and failure energy increased more in the fibrils (40%, 300%, 500%) than fascicles (25%, 150%, 380%), while the relative increase in failure strain was similar (~100%). A detail worth noticing is that the MG treated fascicles had a longer toe region (Fig. 2B), which we suspect is a result of increased bending stiffness of collagen fibers causing force to rise earlier during re-alignment. Toe region length can be estimated by extrapolating the linear part of the curve down to the strain-axis, which yields 0.3% for the controls and 2.4% for the MG treated, so at least part of the increase in failure strain can be attributed to this increased toe region length.

A previous study reported similar mechanical changes at the fascicle level but found no effect on the stiffness or modulus of the fibril [37]. Cross-linking is expected to mainly affect molecular sliding [37,49] and consequently have a greater effect on failure properties than on the first peak in modulus, which is achieved before sliding begins. Although peak modulus increased in the present work, it does not disagree with this theory since the effect was seven times smaller than that on failure stress.

The majority of the MG treated fibrils displayed a third phase of increasing stiffness in the stress-strain response, which was absent in the majority of the controls. This behavior was related to fibril strength with the strongest controls displaying it and the weakest MG treated lacking it (Fig. S4 in Supplement). We have previously observed a very similar mechanical response in collagen fibrils from human patellar tendon compared to fibrils from rat tail tendon [31]. We originally proposed that these differences were due to higher concentrations of mature enzymatic pyridinoline cross-links in human tendons compared to rat tails. The concentration of AGE cross-links was also greater in the human tendons, but we initially surmised that AGE cross-links were less likely to cause the mechanical differences, in part because the human tissue was from young men (~35 years) and in part because we expected the more random nature of AGE cross-linking to result in uniform stiffening rather than distinct phases. In contrast, enzymatic cross-links occur at the telopeptide ends where unfolding of a particular "hairpin loop" could explain the plateau of low stiffness before the third phase [50]. However, in light of the current results on MG treatment and the lack of differences in fibril mechanics related to differences in acid solubility and HP concentration, it seems

likely that AGEs may have played a greater role in the previously observed mechanical behavior of human collagen fibrils, even at a relatively young age. Note that the present study induced a supraphysiological level of MG derived AGE cross-links, whereas the glucose derived AGE cross-link glucosepane is likely more important in vivo. Whether the effects of a physiological level of glucose AGEs are similar remains to be tested.

That the unspecific formation of AGE cross-links result in three mechanical phases, rather than uniform stiffening, indicates that this is an inherent feature of collagen mechanics independent on the specific cross-link site. This is supported by molecular simulations of fibril mechanics, which have reported a similar three-phase behavior where the plateau phase was due to molecular slippage and the final region of high modulus resulted from the end of uncoiling and beginning of backbone stretching within collagen molecules [51,52]. The simulation study also found that trivalent cross-links reinforced the fibril more strongly than divalent ones [51], but in the present work the higher levels of trivalent pyridinoline cross-links in Achilles did not appear to affect fibril mechanics, however, possible differences in other trivalent cross-links are unknown. It should be noted that the important factor is the total number of neighboring molecules connected by the cross-links, and trivalent cross-links may connect the same set of molecules as the divalent ones. Since MG derived cross-links can occur at many sites along the fibril, their effective valence can be higher, possibly explaining the greater mechanical influence.

### 4.3. Fibril structure-mechanics relationship

Fibril diameter has been suggested to affect mechanical properties, and there is some evidence of this at the macroscopic level [53,54]. At the fibril level a reduction in yield stress with increasing fibril volume has also been reported [55]. Some of the proposed mechanisms relate to higher levels of the hierarchy, such as reduced sliding of small fibrils due to larger relative surface area, but others relate to the fibril itself. It has been proposed that large fibrils would be stiffer and stronger due to fewer cross-linking sites being "wasted" on the surface [54], however, the opposite could also be true if the chemical modifications required for cross-linking occur more easily at the surface. A related observation is the possible existence of a core-shell structure in fibrils [56], although other reports have not supported this notion [57]. In the present data there was a negative correlation between diameter and stress-related mechanical parameters (failure stress, peak modulus) when all group differences were accounted for (Fig. 5B). MG treatment may have limited penetration into the fibrils, which could drive this correlation via relatively higher cross-linking of thinner fibrils. Analyzing the treated and control samples separately did not reveal a significant relation to diameter in either group, and in Fig. 5B the two groups also appear to behave similarly. A relation between stress and diameter could be driven by errors in the AFM based diameter measurement. However, artifacts in AFM usually overestimate the dimensions leading to underestimated stress values, and this error would be relatively greater for small fibrils. The AFM based error would therefore result in increasing stress with diameter, contrary to our results. Overall there is some evidence for a reduction of mechanical properties with increasing fibril diameter, but the low correlation coefficient and the fact that it is not significant within treatment groups separately weakens this conclusion.

### 4.4. Local fibril strain

A key advantage of the new mechanical test system is the ability to observe the fibril with light microscopy during mechanical testing, which enables the use of local strain markers to determine strain distribution. While there was some variation in strain along the fibril it was generally uniform except for the ends where strain was consistently higher than in the central part. The strain at failure was 1.7% greater (11% relative increase) in the region where rupture occurred. To determine if there was a consistent strain concentration at the rupture site, the strain difference at 75% of the failure load was also determined, but there was no conclusive evidence for an inherent weakness ($p = 0.19$). Electron microscopy has previously been used to show the existence of local regions of disruption in collagen fibrils following mechanical damage [39] and we had hypothesized that this mechanism could give rise to local regions of increased strain, however, such strain concentration was not clear from the data. It is possible that fibril strain is simply uniform, and the structures observed with electron microscopy are not caused by an inherent property of the fibrils but may result from stress concentrations due to uneven stress transmission from the surrounding matrix. Alternatively, the disrupted regions may only have a small effect on strain and the observed variation of a few percent could represent these regions. It is also possible that the distance between the beads in the present work (25–100 μm) is large enough that each such range stretches over several regions of localized strain concentrations, thereby averaging them out.

### 4.5. Overall fibril mechanics

To our knowledge, the three-phase behavior has only been reported experimentally by our group [31]; however, the present study reproduced this observation by using substantially different equipment and sample preparations than previously. We believe this supports the validity of the observation.

In absolute terms the results are in the same range as our previous studies using AFM, but we generally obtain lower values of stress, strain and modulus than previously. The most comparable data is between the present 16 week old untreated tail fibrils and the rat tail fibrils in Svensson et al. [31], where the failure stress, failure strain and peak modulus were 250 MPa, 17% and 2.6 GPa respectively, compared to the present 80 MPa, 8.9% and 1.6 GPa (using optical strain). While technical sources of error may play a role, we suspect that an important part of the difference is due to the very short fibril segments tested previously (~35 μm) compared to the present study (~270 μm) since the probability of having a local weakness along the fibril increases with length (i.e. the chain not being stronger than the weakest link) [58]. This may also be part of the reason for the large variation in failure stress (Fig. 4E).

For comparison to the fascicle level, the estimated swelling on hydration (~30%) [59] and volume fraction of hydrated fibrils within a hydrated tail tendon (~75%) can be taken into account [60]. Since there were no significant differences between age groups and tissue types the average across all the untreated samples is used: 110 MPa failure stress, and 1.8 GPa peak modulus (using optical strain), which is then equivalent to 50 MPa and 0.8 GPa at the fascicle level. These represent upper bounds on the values achievable in fascicles if no additional strain and failure mechanisms were present between the fibril and fascicle levels. The fact that the measured fascicle modulus exceeds the upper bound expected from the fibril measurements indicates an underestimate at the fibril level. Based on our findings, a possible explanation is the previously mentioned decrease with diameter (Fig. 5B) causing an underestimate of stress and modulus due to the lack of small diameter fibrils in our data. Another factor may be a general overestimate of fibril diameter in AFM images.

### 4.6. Limitations

An important limitation in this study is the drying/rehydration of fibrils required for sample preparation, which may affect the

mechanical properties. To shed some light on this we examined the acid solubility and mechanical properties of tail fascicles after 1 week of drying followed by rehydration. Acid solubility decreased and peak modulus, failure stress and failure strain increased, but the effects were insufficient to obscure the underlying age differences, suggesting that drying alone cannot explain the lack of differences at the fibril level (details in Supplement S2.2). A recent study has focused on preparing fibril samples fully hydrated, but to our knowledge the optical trap utilized cannot achieve sufficient load for a failure test [61]. The long storage period before fibril testing could also be an issue, however, the fascicle mechanics in supplement S2.2 were recorded after fibril testing and still displayed the age differences seen in the original tests. In addition, a recent study found no mechanical effects at the micro scale after frozen storage of tail tendon for up to 6 months [62]. None the less, the effects of long term frozen storage on fibril mechanics remain an unknown factor, which could affect our results.

Another limitation is an inherent selection bias of the tested fibrils. First, there is a size bias because fibrils are located with an optical microscope, making it largely impossible to test fibrils below 80 nm. Second, there is a potential overestimate of fibril strength since weaker fibrils are more likely to break during preparation, thereby never completing the mechanical test. This is supported by the observation that 58% the mechanically weaker control fibrils and only 39% of the MG treated fibrils broke during preparation, however, there was less difference between young (57%) and old (44%) as well as tail (53%) and Achilles (50%). It therefore seems unlikely that the mechanical bias affected the comparison of maturation and tissue type substantially.

Only pyridinoline cross-links were directly measured and while acid solubility may serve as an indicator of labile aldimine cross-links, it is not possible to assess changes in other cross-links, including immature ketoamine as well as mature pyrrole and histidine derived cross-links [27]. General conclusions regarding enzymatic cross-linking are therefore tentative.

A final limitation is the lack of viscoelastic mechanical tests such as stress-relaxation or creep, which could be more sensitive to some mechanical changes [37]. We were unable to perform such tests with our equipment because the dynamic range is limited by high frequency noise above 30 Hz and low frequency fluctuations over several seconds (details in Supplement S1.2).

## 5. Conclusion

Counter to our initial hypotheses, the level of mature pyridinoline cross-linking had little to no effect on fibril mechanics. AGE induction with MG did increase fibril strength and stiffness as expected, but also increased ultimate strain leading to stronger and tougher fibrils rather than more brittle ones. There was an increased local strain near the rupture site of the fibrils, but the difference was relatively small and, within experimental variations, the overall strain was evenly distributed over the fibril length. Also counter to expectations, AGE induction did not affect the uniformity of local strains. Finally, AGE treatment resulted in a three-phase mechanical response very similar to what has previously been seen in young adult human tendons, suggesting that AGEs may play an important mechanical role in human tendons, even before old age.

## Acknowledgements

We thank the following for their assistance in the project: Søren Munk Ribel-Madsen for expert assistance with HPLC measurements. Reuben Howden for assistance and access to lab facilities at UNC Charlotte. Kaleb Templeton for assistance with testing and developing the nanomechanical device. The Core Facility for Integrated Microscopy, Faculty of Health and Medical Sciences, University of Copenhagen, for access to microscopy equipment. The Nano-Science Center, Faculty of Science, University of Copenhagen, for access to atomic force microscopy.

## Funding

The study was funded by the Danish Council for Independent Research: Medical Sciences (DFF-1333-00052A). The Institute of Sports Medicine Copenhagen received funding from the Lundbeck Foundation (R198-2015-207), the Novo Nordisk Foundation, the Danish Council for Independent Research: Medical Sciences (FSS 4183-00023B) and the Center for Healthy Aging. The funding bodies had no influence on the study.

## Disclosures

All authors declare no conflicting interests.

## Contributions

Conception and design: RBS, STS, PJM, SPM. Laboratory work: RBS, STS, PJM. Data analysis: RBS. Interpretation and discussion: RBS, SPM. Review and approval of manuscript: RBS, STS, PJM, SPM.

## Appendix A. Supplementary data

Supplementary data associated with this article can be found, in the online version, at https://doi.org/10.1016/j.actbio.2018.02.005.

## References

[1] K. Gelse, E. Poschl, T. Aigner, Collagens - structure, function, and biosynthesis, Adv. Drug Del. Rev. 55 (2003) 1531–1546.
[2] D.A.D. Parry, A.S. Craig, Quantitative electron microscope observations of collagen fibrils in rat-tail tendon, Biopolymers 16 (1977) 1015–1031.
[3] A.J. Hodge, J.A. Petruska, Recent studies with the electronmicroscope on ordered aggregates of the tropocollagen macromolecule, in: G.N. Ramachandran (Ed.), Aspects of Protein Structure, Academic Press, New York, 1963, pp. 299–300.
[4] P. Bornstein, A.H. Kang, K.A. Piez, The nature and location of intramolecular cross-links in collagen, Proc. Natl. Acad. Sci. U.S.A. 55 (1966) 417–424.
[5] R.C. Siegel, J.C. Fu, Collagen cross-linking. Purification and substrate specificity of lysyl oxidase, J. Biol. Chem. 251 (1976) 5779–5785.
[6] S.R. Pinnell, G.R. Martin, The cross-linking of collagen and elastin: enzymatic conversion of lysine in peptide linkage to alpha-aminoadipic-delta-semialdehyde (allysine) by an extract from bone, Proc. Natl. Acad. Sci. U.S.A. 61 (1968) 708–716.
[7] D.J. Cannon, P.F. Davison, Crosslinking and aging in rat tendon collagen, Exp. Gerontol. 8 (1973) 51–62.
[8] M.L. Tanzer, Intermolecular cross-links in reconstituted collagen fibrils - evidence for nature of covalent bonds, J. Biol. Chem. 243 (1968) 4045–4054.
[9] G.L. Mechanic, Y. Kuboki, H. Shimokawa, K. Nakamoto, S. Sasaki, Y. Kawanishi, Collagen crosslinks: direct quantitative determination of stable structural crosslinks in bone and dentin collagens, Biochem. Biophys. Res. Commun. 60 (1974) 756–763.
[10] C. Henning, M.A. Glomb, Pathways of the maillard reaction under physiological conditions, Glycoconj. J. 33 (2016) 499–512.
[11] P.J. Thornalley, Protein and nucleotide damage by glyoxal and methylglyoxal in physiological systems – role in ageing and disease, Drug Metabol. Drug Interact. 23 (2008) 125–150.
[12] D.R. Sell, K.M. Biemel, O. Reihl, M.O. Lederer, C.M. Strauch, V.M. Monnier, Glucosepane is a major protein cross-link of the senescent human extracellular matrix. Relationship with diabetes, J. Biol. Chem. 280 (2005) 12310–12315.
[13] K.M. Biemel, D.A. Friedl, M.O. Lederer, Identification and quantification of major maillard cross-links in human serum albumin and lens protein. Evidence for glucosepane as the dominant compound, J. Biol. Chem. 277 (2002) 24907–24915.
[14] G.T. Mustata, M. Rosca, K.M. Biemel, O. Reihl, M.A. Smith, A. Viswanathan, C. Strauch, Y. Du, J. Tang, T.S. Kern, M.O. Lederer, M. Brownlee, M.F. Weiss, V.M. Monnier, Paradoxical effects of green tea (camellia sinensis) and antioxidant vitamins in diabetic rats: improved retinopathy and renal mitochondrial

defects but deterioration of collagen matrix glycoxidation and cross-linking, Diabetes 54 (2005) 517–526.
[15] K.M. Reiser, M.A. Amigable, J.A. Last, Nonenzymatic glycation of type I collagen. The effects of aging on preferential glycation sites, J. Biol. Chem. 267 (1992) 24207–24216.
[16] A. Gautieri, A. Redaelli, M.J. Buehler, S. Vesentini, Age- and diabetes-related nonenzymatic crosslinks in collagen fibrils: candidate amino acids involved in advanced glycation end-products, Matrix Biol. 34 (2014) 89–95.
[17] V.M. Monnier, O. Bautista, D. Kenny, D.R. Sell, J. Fogarty, W. Dahms, P.A. Cleary, J. Lachin, S. Genuth, Skin collagen glycation, glycoxidation, and crosslinking are lower in subjects with long-term intensive versus conventional therapy of type 1 diabetes: relevance of glycated collagen products versus HbA1c as markers of diabetic complications. DCCT skin collagen ancillary study group. Diabetes control and complications trial, Diabetes 48 (1999) 870–880.
[18] S.P. Robins, M. Shimokomaki, A.J. Bailey, The chemistry of the collagen cross-links. Age-related changes in the reducible components of intact bovine collagen fibres, Biochem. J. 131 (1973) 771–780.
[19] Y. Nakagawa, K. Hayashi, N. Yamamoto, K. Nagashima, Age-related changes in biomechanical properties of the achilles tendon in rabbits, Eur. J. Appl. Physiol. Occup. Physiol. 73 (1996) 7–10.
[20] R.C. Haut, The effect of a lathyritic diet on the sensitivity of tendon to strain rate, J. Biomech. Eng. 107 (1985) 166–174.
[21] N. Verzijl, J. DeGroot, Z.C. Ben, O. Brau-Benjamin, A. Maroudas, R.A. Bank, J. Mizrahi, C.G. Schalkwijk, S.R. Thorpe, J.W. Baynes, J.W.J. Bijlsma, F.P.J.G. Lafeber, J.M. TeKoppele, Crosslinking by advanced glycation end products increases the stiffness of the collagen network in human articular cartilage: a possible mechanism through which age is a risk factor for osteoarthritis, Arthritis Rheum. 46 (2002) 114–123.
[22] G.K. Reddy, Cross-linking in collagen by nonenzymatic glycation increases the matrix stiffness in rabbit achilles tendon, Exp. Diabesity Res. 5 (2004) 143–153.
[23] T.T. Andreassen, K. Seyerhansen, A.J. Bailey, Thermal-stability, mechanical-properties and reducible cross-links of rat tail tendon in experimental diabetes, Biochim. Biophys. Acta 677 (1981) 313–317.
[24] G.L. Cheing, R.M. Chau, R.L. Kwan, C.H. Choi, Y.P. Zheng, Do the biomechanical properties of the ankle-foot complex influence postural control for people with type 2 diabetes?, Clin Biomech. 28 (2013) 88–92.
[25] A.D. Gonzalez, M.A. Gallant, D.B. Burr, J.M. Wallace, Multiscale analysis of morphology and mechanics in tail tendon from the ZDSD rat model of type 2 diabetes, J. Biomech. 47 (2014) 681–686.
[26] R.B. Svensson, K.M. Heinemeier, C. Couppe, M. Kjaer, S.P. Magnusson, Effect of aging and exercise on the tendon, J. Appl. Physiol. 121 (2016) 1237–1246.
[27] A.J. Bailey, R.G. Paul, L. Knott, Mechanisms of maturation and ageing of collagen, Mech. Ageing Dev. 106 (1998) 1–56.
[28] S.J. Eppell, B.N. Smith, H. Kahn, R. Ballarini, Nano measurements with micro-devices: mechanical properties of hydrated collagen fibrils, J. R. Soc. Interface 3 (2006) 117–121.
[29] J.A.J. van der Rijt, K.O. van der Werf, M.L. Bennink, P.J. Dijkstra, J. Feijen, Micromechanical testing of individual collagen fibrils, Macromol. Biosci. 6 (2006) 697–702.
[30] L. Yang, K.O. van der Werf, B. Koopman, V. Subramaniam, M.L. Bennink, P.J. Dijkstra, J. Feijen, Micromechanical bending of single collagen fibrils using atomic force microscopy, J. Biomed. Mater. Res. A 82A (2007) 160–168.
[31] R.B. Svensson, H. Mulder, V. Kovanen, S.P. Magnusson, Fracture mechanics of collagen fibrils: influence of natural cross-links, Biophys. J. 104 (2013) 2476–2484.
[32] B.P. Flynn, G.E. Tilburey, J.W. Ruberti, Highly sensitive single-fibril erosion assay demonstrates mechanochemical switch in native collagen fibrils, Biomech. Model. Mechanobiol. 12 (2013) 291–300.
[33] R.B. Svensson, T. Hassenkam, P. Hansen, S.P. Magnusson, Viscoelastic behavior of discrete human collagen fibrils, J. Mech. Behav. Biomed. Mater. 3 (2010) 112–115.
[34] Z.L.L. Shen, H. Kahn, R. Ballarin, S.J. Eppell, Viscoelastic properties of isolated collagen fibrils, Biophys. J. 100 (2011) 3008–3015.
[35] L. Yang, K.O. van der Werf, P.J. Dijkstra, J. Feijen, M.L. Bennink, Micromechanical analysis of native and cross-linked collagen type I fibrils supports the existence of microfibrils, J. Mech. Behav. Biomed. Mater. 6 (2012) 148–158.
[36] R. Puxkandl, I. Zizak, O. Paris, J. Keckes, W. Tesch, S. Bernstorff, P. Purslow, P. Fratzl, Viscoelastic properties of collagen: synchrotron radiation investigations and structural model, Philos. Trans. R. Soc. Lond., B, Biol. Sci. 357 (2002) 191–197.
[37] G. Fessel, Y. Li, V. Diederich, M. Guizar-Sicairos, P. Schneider, D.R. Sell, V.M. Monnier, J.G. Snedeker, Advanced glycation end-products reduce collagen molecular sliding to affect collagen fibril damage mechanisms but not stiffness, PloS One 9 (2014) e110948.
[38] D.R. Eyre, M.A. Paz, P.M. Gallop, Cross-linking in collagen and elastin, Annu. Rev. Biochem 53 (1984) 717–748.
[39] S.P. Veres, J.M. Harrison, J.M. Lee, Repeated subrupture overload causes progression of nanoscaled discrete plasticity damage in tendon collagen fibrils, J. Orthop. Res. 31 (2013) 731–737.
[40] Y. Li, G. Fessel, M. Georgiadis, J.G. Snedeker, Advanced glycation end-products diminish tendon collagen fiber sliding, Matrix Biol. 32 (2013) 169–177.
[41] S. Yang, J.E. Litchfield, J.W. Baynes, Age-breakers cleave model compounds, but do not break maillard crosslinks in skin and tail collagen from diabetic rats, Arch. Biochem. Biophys. 412 (2003) 42–46.
[42] I. Syk, M.S. Agren, D. Adawi, B. Jeppsson, Inhibition of matrix metalloproteinases enhances breaking strength of colonic anastomoses in an experimental model, Br. J. Surg. 88 (2001) 228–234.
[43] V.M. Monnier, S. Genuth, D.R. Sell, The pecking order of skin advanced glycation endproducts (ages) as long-term markers of glycemic damage and risk factors for micro- and subclinical macrovascular disease progression in type 1 diabetes, Glycoconj. J. 33 (2016) 569–579.
[44] V.M. Monnier, V. Vishwanath, K.E. Frank, C.A. Elmets, P. Dauchot, R.R. Kohn, Relation between complications of type I diabetes mellitus and collagen-linked fluorescence, N. Engl. J. Med. 314 (1986) 403–408.
[45] B.T. Fokkens, A.J. Smit, Skin fluorescence as a clinical tool for non-invasive assessment of advanced glycation and long-term complications of diabetes, Glycoconj. J. 33 (2016) 527–535.
[46] D. Brown, Tracker video analysis and modeling tool, vers. 4.72, <http://physlets.org/tracker/>, (accessed December 12, 2012).
[47] R.B. Svensson, P. Hansen, T. Hassenkam, B.T. Haraldsson, P. Aagaard, V. Kovanen, M. Krogsgaard, M. Kjaer, S.P. Magnusson, Mechanical properties of human patellar tendon at the hierarchical levels of tendon and fibril, J. Appl. Physiol. 112 (2012) 419–426.
[48] K. Legerlotz, G.P. Riley, H.R.C. Screen, Specimen dimensions influence the measurement of material properties in tendon fascicles, J. Biomech. 43 (2010) 2274–2280.
[49] M.J. Buehler, Nanomechanics of collagen fibrils under varying cross-link densities: atomistic and continuum studies, J. Mech. Behav. Biomed. Mater. 1 (2008) 59–67.
[50] S.G.M. Uzel, M.J. Buehler, Molecular structure, mechanical behavior and failure mechanism of the C-terminal cross-link domain in type I collagen, J. Mech. Behav. Biomed. Mater. 4 (2011) 153–161.
[51] B. Depalle, Z. Qin, S.J. Shefelbine, M.J. Buehler, Influence of cross-link structure, density and mechanical properties in the mesoscale deformation mechanisms of collagen fibrils, J. Mech. Behav. Biomed. Mater. 52 (2015) 1–13.
[52] M.J. Buehler, Atomistic and continuum modeling of mechanical properties of collagen: elasticity, fracture, and self-assembly, J. Mater. Res. 21 (2006) 1947–1961.
[53] K.L. Goh, D.F. Holmes, Y. Lu, P.P. Purslow, K.E. Kadler, D. Bechet, T.J. Wess, Bimodal collagen fibril diameter distributions direct age-related variations in tendon resilience and resistance to rupture, J. Appl. Physiol. 113 (2012) 878–888.
[54] D.A.D. Parry, The molecular and fibrillar structure of collagen and its relationship to the mechanical properties of connective tissue, Biophys. Chem. 29 (1988) 195–209.
[55] Z.L. Shen, M.R. Dodge, H. Kahn, R. Ballarini, S.J. Eppell, Stress-strain experiments on individual collagen fibrils, Biophys. J. 95 (2008) 3956–3963.
[56] T. Gutsmann, G.E. Fantner, M. Venturoni, A. Ekani-Nkodo, J.B. Thompson, J.H. Kindt, D.E. Morse, D.K. Fygenson, P.K. Hansma, Evidence that collagen fibrils in tendons are inhomogeneously structured in a tubelike manner, Biophys. J. 84 (2003) 2593–2598.
[57] M.P.E. Wenger, M.A. Horton, P. Mesquida, Nanoscale scraping and dissection of collagen fibrils, Nanotechnology 19 (2008) 384006.
[58] Z.P. Bazant, Scaling theory for quasibrittle structural failure, Proc. Natl. Acad. Sci. U.S.A. 101 (2004) 13400–13407.
[59] K.M. Meek, N.J. Fullwood, P.H. Cooke, G.F. Elliott, D.M. Maurice, A.J. Quantock, R.S. Wall, C.R. Worthington, Synchrotron x-ray diffraction studies of the cornea, with implications for stromal hydration, Biophys. J. 60 (1991) 467–474.
[60] K.L. Goh, D.F. Holmes, H.Y. Lu, S. Richardson, K.E. Kadler, P.P. Purslow, T.J. Wess, Ageing changes in the tensile properties of tendons: influence of collagen fibril volume fraction, J. Biomech. Eng. 130 (2008) 021011.
[61] P. Dutov, O. Antipova, S. Varma, J.P.R.O. Orgel, J.D. Schieber, Measurement of elastic modulus of collagen type I single fiber, PloS one 11 (2016) e0145711.
[62] A.H. Lee, D.M. Elliott, Freezing does not alter multiscale tendon mechanics and damage mechanisms in tension, Ann. N. Y. Acad. Sci. 1409 (2017) 85–94, https://doi.org/10.1111/nyas.13460.